CLASSIFICATION OF PATHOGENIC BACTERIA USING NEAR-INFRARED DIFFUSE REFLECTANCE SPECTROSCOPY

Pin Wang [1*], Jie Wang [1], Lirui Wang [1], Meifang Yin [2], Yongming Li [1], Jun Wu [3*]

[1] College of Communication Engineering, Chongqing University, Chongqing, 400044, China; e-mail: wangpin@cqu.edu.cn
[2] Institute of Burn Research, Southwest Hospital, Third Military Medical University, Chongqing 400038, China
[3] The First Affiliated Hospital Sun Yat-Sen University, Department of Burns, Guangzhou 510080, China; e-mail: junwupro@126.com

Near-infrared diffuse reflectance spectroscopy is proposed for the classification of pathogenic bacteria using optical properties. The spectrally resolved data are analyzed using a diffuse reflectance model to extract the local optical properties, including the reduced scattering coefficient and absorption coefficient. The optical properties at different wavelengths form the feature set. A particle swarm optimization-based support vector machine is used to classify seven categories of bacteria. The experimental results demonstrate the feasibility of the method for the rapid and noninvasive classification of pathogenic bacteria using optical properties.

Keywords: *pathogenic bacteria, optical properties, near-infrared diffuse reflectance spectroscopy, particle swarm optimization, support vector machine.*

КЛАССИФИКАЦИЯ ПАТОГЕННЫХ БАКТЕРИЙ С ИСПОЛЬЗОВАНИЕМ СПЕКТРОСКОПИИ ДИФФУЗНОГО ОТРАЖЕНИЯ В БЛИЖНЕМ ИНФРАКРАСНОМ ДИАПАЗОНЕ

P. Wang [1*], J. Wang [1], L. Wang [1], M. Yin [2], Y. Li [1], J. Wu [3*]

УДК 543.42

[1] Колледж связи, Чунцинский университет, Чунцин, 400044, Китай; e-mail: wangpin@cqu.edu.cn
[2] Институт ожоговых исследований, Чунцин, 400038, Китай
[3] Первая больница при Университете Сунь Ят-Сена, Гуанчжоу, 510080, Китай; e-mail: junwupro@126.com

(Поступила 5 мая 2017)

Для классификации патогенных бактерий предложено использовать их оптические свойства, полученные с помощью спектроскопии диффузионного отражения в ближнем ИК диапазоне. Спектральные данные анализируются на основе модели диффузного отражения с целью установления коэффициентов рассеяния и поглощения для различных длин волн. Для классификации семи категорий бактерий использован метод опорных векторов, основанный на оптимизации роя частиц. Продемонстрирована возможность применения метода на основе оптических свойств для быстрой и неинвазивной классификации патогенных бактерий.

Ключевые слова: *патогенная бактерия, оптические свойства, спектроскопия диффузного отражения в ближней ИК области, метод роя частиц, метод опорных векторов.*

Introduction. A burn wound can be caused by exposure to heat, electricity, radiation, and chemicals [1]. A burn wound is mostly an open wound, so bacterial colonization is unavoidable because of the presence of a large number of necrotic and degenerative tissues [2–4]. When bacteria are confined to surface exudates or liquefied necrotic tissues, they have little effect on the entire body. However, if they invade adjacent living tissues and reach a certain number, then there will be systemic symptoms, commonly known as a “burn

wound invasive infection" or "burn wound sepsis" [5–7]. Therefore, early diagnosis of wound infection and the use of proper antibiotics is essential for treatment.

The prerequisite for the diagnosis of a wound infection is the classification and discrimination of bacteria. There are few studies on the classification of burn wound bacteria. Hence, the seven categories of pathogenic bacteria which are most common in burn wound infection will be discussed in this paper. Conventional methods for the classification of bacteria mainly rely on specific microbiological and biochemical identification [8, 9]. The present gold standard, that is, the culture-based method, is highly reliable but requires days for preliminary results. Some modern biotechnology detection methods, such as the polymerase chain reaction method, gene chip technology, microarray technology, and other analytical methods, have been widely investigated [10–12]. Although these methods can be sensitive and robust, they are complicated, expensive, and require professional operators. The aforementioned methods have limitations in clinical application. Therefore, there is an urgent need to establish a rapid, simple, noninvasive, and effective method for the classification of pathogenic bacteria.

Various noninvasive optical approaches have been studied for detecting infected bacterial cells [13, 14]. Spectroscopy technologies for the rapid identification of the bacteria suspension has become very popular [15, 16]. Among these methods, Fourier transform infrared spectroscopy has been extensively investigated [17, 18]. Typically, principal component analysis is applied to extract spectral features for the identification of bacteria [19, 20]. Light scattering technology has been investigated for bacterial classification [21, 22]. A number of features of the scattering pattern have been extracted for analysis and classification. However, for previous optical technologies, the extracted features are not physically meaningful and lack information on the structural characteristics of bacteria. For near-infrared diffuse reflectance spectroscopy (NIDRS), light delivered to the sample undergoes multiple elastic scattering and absorption, and part of it returns as diffuse reflectance carrying quantitative information about the sample structure and composition. Optical properties related to scattering and absorption characterize the structural components of different pathogenic bacteria well. They reveal the internal structure and composition of the bacteria suspension and explore the essential differences of different bacteria. Therefore, they can be used to distinguish different types of burn wound bacteria in the physical sense.

In this study, an efficient, noninvasive NIDRS-based method is proposed for rapidly classifying burn wound bacteria using the optical properties of the bacteria suspension. An in-depth analysis of the optical properties reveals the internal structure and composition of the bacteria and explores the essential differences between the different types of pathogenic bacteria. The validity of optical properties for pathogenic bacteria classification is demonstrated using a support vector machine (SVM) classification method optimized using particle swarm optimization (PSO). The specific procedures are outlined as follows: (1) an NIDRS system is developed to collect the diffuse reflectance spectrum; (2) a diffuse reflectance model is used to extract the optical parameters: reduced scattering coefficient (μ_s') and absorption coefficient (μ_a); (3) an SVM is applied to classify the bacteria; and (4) a PSO algorithm is used to optimize the parameters of the SVM model, and the independent samples are used to test the model.

Experiment. The strains of burn wound bacteria were obtained from the Microbiology Laboratory of Burn Institute, Southwest Hospital, Third Military Medical University. The seven categories of bacteria were Staphylococcus aureus (Sau, ATU25923), Escherichia coli (Eco, ATU25922), Enterococcus faecalis (Efa, 201511199), Proteus vulgaris (Pvu, 201511208), Klebsiella pneumoniae (Kpn, 201512054), Acinetobacter baumannii (Aba, 201512065), and Pseudomonas aeruginosa (Pae, 201512043).

The strains of bacteria were grown on a CAN agar plate. A few tips of solid-cultured bacterial colonies were taken and then put into tubes with LB broth. Bacteria were grown in 20 mL LB broth for 12 h in a shaker incubator at 37°C. The optical density of the bacteria after 12 h growth was measured. Bacteria were diluted in LB broth prior to the experiments, with an inoculation concentration of 10^9 cfu/mL. There were three samples for each category of bacteria. To ensure that the concentration of bacteria to be tested was the same, the bacterial concentration was calibrated by the optical density value. The number of NIDRS samples for each category of bacteria was approximately 750.

A diffuse reflectance spectroscopy system was developed and used for the measurement of the bacteria suspension. Broad light from a tungsten halogen lamp (Ocean Optics HL 2000) was delivered to the bacteria suspension via an emitting optical fiber within a fiber optic probe (Ocean Optics QP600-2). A collecting fiber adjacent to the emitting fiber collected emitted light and delivered it to a spectrometer (Ocean Optics NIR-Quest) with a range of 900–2500 nm and spectral resolution of 4.6 nm at FWHM. The obtained diffuse reflectance spectrum was calculated as

$$R(\lambda) = \frac{I_s(\lambda) - I_{bg}(\lambda)}{I_{ref}(\lambda) - I_{bg}(\lambda)}, \quad (1)$$

where $R(\lambda)$ is the normalized signal, $I_s(\lambda)$ is the broadband light intensity measured from the bacteria sample, $I_{bg}(\lambda)$ is a background spectrum recorded with the light source turned off, and I_{ref} is a measured spectrum from a reflectance standard. Subtracting the dark spectrum eliminated the effects of CCD dark current and ambient light, whereas a wavelength-dependent system response was eliminated by normalizing the sample response to a reflectance standard.

Figure 1 shows a representative original near-infrared diffuse reflectance spectrum $R(\lambda)$ for the seven categories of bacteria. It can be seen that the spectrum is almost overlapping, and it is difficult to classify the bacteria based on the original NIDRS data. Then, we extracted optical properties to classify pathogenic bacteria.

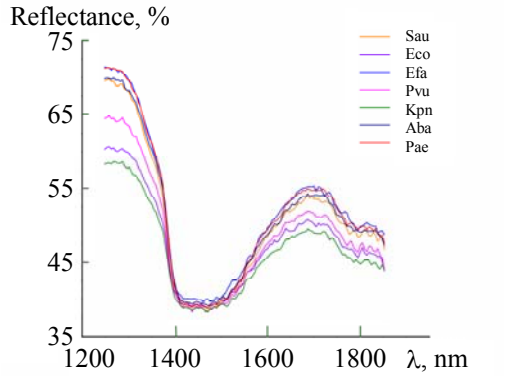

Fig. 1. Representative original near-infrared diffuse reflectance spectra for the seven categories of bacteria.

Calculation of the optical properties. Two optical properties, the reduced scattering coefficient μ_s' and absorption coefficient μ_a, were calculated using the diffuse reflectance model. The diffuse reflectance spectrum expression is described as [23]

$$R_p(\lambda) = \frac{\mu_s'}{\mu_s' + \mu_a}\left\{\exp(-\mu z_0) + \exp\left[-\left(1+\frac{4}{3}B\right)\mu z_0\right] - z_0\frac{\exp(-\mu r_1')}{r_1'} - \left(1+\frac{4}{3}B\right)z_0\frac{\exp(-\mu r_2')}{r_2'}\right\}, \quad (2)$$

with $z_0 = 1/(\mu_s' + \mu_a)$, $r_1' = (z_0^2 + r_c^2)^{1/2}$, $r_2' = [z_0^2(1 + 4B/3)^2 + r_c^2]^{1/2}$, and $\mu = [3\mu_a(\mu_a + \mu_s')]^{1/2}$, where r_c is the radius of the light collection area. Parameter B depends on refractive index n of the medium ($B = 3.2$). In Eq. (2), the values of B and r_c are fixed. The sum of squared error between $R_p(\lambda)$ and the original measured diffuse spectral data $R(\lambda)$ at each wavelength was minimized to obtain optical properties μ_s' and μ_a at each wavelength.

Figure 2 shows the reflectance spectra obtained with the NIDRS and the corresponding fitted spectra. A good fit was achieved for a wide range of wavelengths. The results show that the extraction of optical properties was conducted under reasonable conditions.

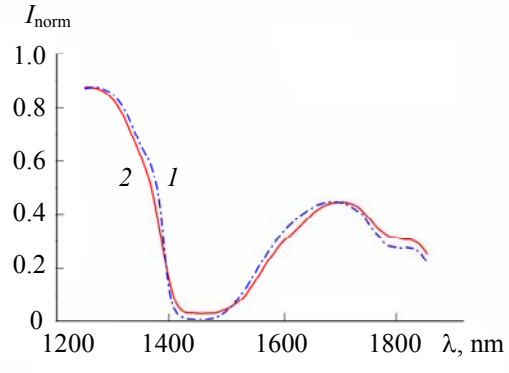

Fig. 2. Representative reflectance spectra of the fitted model (1) and corresponding original spectral data (2).

Particle swarm optimization-based support vector machine. SVMs have been widely applied in the classification of bacteria. Therefore, an SVM classifier was used in the study [24]. There are four kernel functions of an SVM. In study, the most commonly used three functions, linear, polynomial, and radial basis function (RBF), were selected for comparison.

Suppose training set (optical properties) $X = \{(\mu_s')^n, (\mu_a)^n\}$, $n = 1, ..., 7$, where n is the category of burn wound bacteria. Add labels to each type of pathogenic bacteria. The resulting labels are $Y = \{y^n\}$, $y = 1, ..., 7$, then, $\{X, Y\} = \{(x_i, y_i) | i = 1, 2, ..., N\}$, where x_i is a feature vector, y_i is a label for x_i, and N is the total number of training samples for the seven categories of bacteria. The optimal hyperplane can be obtained using

$$\begin{cases} \max\limits_{\lambda} \left(\sum\limits_{i} \lambda_i - \dfrac{1}{2} \sum\limits_{i,j} \lambda_i \lambda_j y_i y_j K\left(x_i, x_j\right) \right) \\ s.t. \quad 0 \le \lambda_i \le C, \quad i = 1, 2, \cdots, N \\ \qquad \sum\limits_{i=1}^{N} \lambda_i y_i = 0 \end{cases} \tag{3}$$

$$f(x) = \sum_{i=1}^{N_s} \lambda_i y_i K\left(x, x_i\right) + b, \tag{4}$$

where $f(x)$ is the classification function for the SVM algorithm, x is the test sample, λ_i is the optimal Lagrange operator, bias b is computed by calculating the mean values under all conditions, and N_s is the number of support vectors. As we know, in kernel function $K(x, x_i)$, C is the optimizing parameter for linear, polynomial and RBF kernel functions, and γ is only related to the RBF kernel function; C and γ are parameters that influence the classification and generalization ability of the SVM model, so the PSO algorithm was introduced to obtain the optimal SVM parameters.

PSO is a population-based global optimization technique. In PSO, each value of C and γ is described as a "particle," which presents a potential solution to each optimization problem [25].

Suppose that particles are treated as points in D-dimensional space with a certain velocity. D-dimensional space represents the Euclidean space formed by the variables. By calculating the values of the fitness function of particles, the optimal position in the population is represented as g, and also known as g_{best}. For each generation, the d-dimensional ($1 \le d \le D$) velocity and position are varied according to

$$v_{id}^k = w v_{id}^{k-1} + c_1 \, \mathrm{rand}_1 (p_{id}^{k-1} - x_{id}^{k-1}) + c_2 \, \mathrm{rand}_2 (p_{gd}^{k-1} - x_{id}^{k-1}), \tag{5}$$

$$x_{id}^k = x_{id}^{k-1} + \zeta v_{id}^k, \tag{6}$$

where w is the inertia weight; c_1 and c_2 are learning factors, typically set to be 2; rand_1 and rand_2 are random numbers uniformly distributed in [0, 1]; v_{id}^k and x_{id}^k are the dth dimension flight velocity vector and position vector of particle X_i at iteration k, respectively; p_{id}^k and p_{gd}^i are the best values currently and among all particles in the population, respectively; and ζ is a constant coefficient.

In this study, the SVM classification error was used as the fitness function to calculate the fitness of each particle. The particle with the lowest fitness function value is the optimal solution [25]. PSO was used to optimize SVM parameters C and γ. The PSO process is described as follows. 1) Initialize a group of particles (C and γ), including the random position and velocity. 2) Encode the parameters of SVM in binary code, and then call the SVM algorithm for training and testing, thereby evaluating the fitness value of each particle based on the classification error. 3) For each particle, compare its fitness value with the optimal position, and if it is better, it becomes the current best position. 4) Adjust the particle velocity and position according to Eqs. (5) and (6). 5) If the iterative condition is reached, then the current optimal parameters C and γ are output. Otherwise, return to Step 2.

The classification process for burn wound bacteria with the optimized SVM is shown in Fig. 3, and the steps of the process are as follows:

Step 1: Input original NIDRS data.

Step 2: Data preprocessing. Apply the Savitzky–Golay filter to eliminate noise in the original NIDRS data.

Step 3: Extract the optical properties from the original diffuse spectral data using the diffuse reflectance model.

Step 4: Use the resulting optical properties μ_s' and μ_a to form a feature set and input the feature set into the initialized classification model.

Step 5: Binary code parameters C and γ of the SVM into particles. Optimize SVM parameters C and γ using PSO based on the formed feature set. Use the optimized SVM to classify the seven types of bacteria, where the classification error value is the fitness value. If the fitness value satisfies the set error precision or reaches the maximum iteration number, go to Step 6; otherwise, go to Step 5.
Step 6: Update the velocity and position of all the particles according to Eqs. (5) and (6).
Step 7: When the termination conditions are met, output the obtained optimization parameters C and γ.

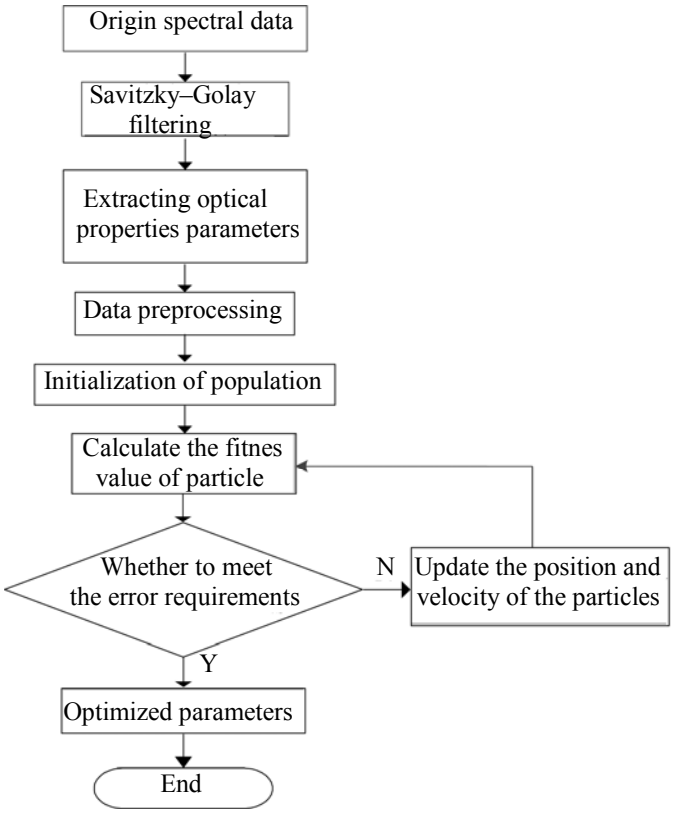

Fig. 3. Classification process of burn wound bacteria with the optimized SVM.

Results and discussion. The number of NIDRS samples for each category of bacteria was approximately 750. The Savitzky–Golay filter was applied to eliminate noise from the original NIDRS data. After data preprocessing, the optical properties of bacteria were obtained using the fitting algorithm. According to the performance of the system, the spectrum of 1.280–1.620 nm was selected for analysis.

The values of optical properties μ_a and μ_s' are shown in Fig. 4. Figure 4a illustrates the value of absorption coefficient μ_a at each wavelength for seven categories of bacteria. The absorption coefficient (μ_a) is directly related to the concentration of absorbers in the bacteria suspension. As can be seen, generally, the value of μ_a reached its peak at 1450 nm. μ_a values for Efa, Pae, Sau, and Aba were almost the same, and those for three other categories of bacteria were different. As seen in Fig. 4b, the value of reduced scattering coefficient μ_s' decreased with an increasing wavelength. The difference in μ_s' values between Pae, Sau, and Aba was negligible and that between Efa, Pvu, Eco, and Kpn decreased in turn. The reduced scattering coefficient (μ_s') reflects the size and density of scatterers in the bacteria suspension. Figure 4 illustrates that Pae, Sau, and Aba had a similar concentration of absorbers and size and density of scatteres; thus, the classification of the three bacteria was difficult. The values of μ_a and μ_s' varied for different wavelengths and bacteria, which indicates that the optical properties can be used to classify the bacteria.

Table 1 shows the values of μ_s' and μ_a, and standard deviation of the seven categories of pathogenic bacteria at a center wavelength of 1450 nm. It demonstrates that the optical properties of Sau, Aba, and Pae were very close, their structure and composition were analogous, and the three bacteria were difficult to distinguish.

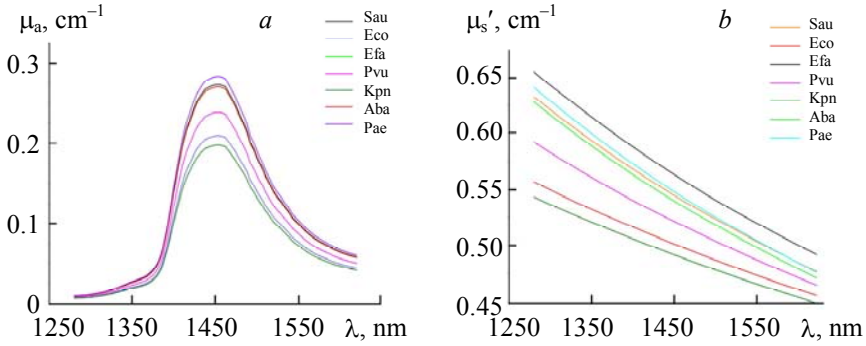

Fig. 4. Absorption coefficient μ_a and reduced scattering coefficient μ_s' at each wavelength for seven categories of bacteria.

TABLE 1. Values μ_s' and μ_a for the Seven Categories of Pathogenic Bacteria at Wavelength 1450 nm

Bacteria	Sau	Eco	Efa	Pvu	Kpn	Aba	Pae
μ_s', cm^{-1}	0.545±0.002	0.501±0.004	0.563±0.005	0.521±0.001	0.491±0.013	0.539±0.006	0.548±0.0068
μ_a, cm^{-1}	0.274±0.002	0.209±0.004	0.271±0.005	0.238±0.004	0.198±0.007	0.271±0.004	0.284±0.004

Figure 5 shows the scatter plot of the values of the absorption and reduced scattering coefficient at 1450 nm for the seven categories of bacteria. It can be seen that Efa, Pae, Sau, and Aba merged and were difficult to separate. The other three categories were well separated and could easily be distinguished. This further demonstrated that the optical properties using diffuse reflectance spectroscopy could be applied for bacteria classification.

The obtained optical properties parameters μ_a and μ_s' of different wavelengths formed a feature set that was used to classify bacteria. The total number of spectra samples for seven categories of bacteria was 5299. Two-thirds of the samples were chosen randomly as training samples, and the remaining samples were used for testing. An SVM was chosen as the classifier to verify the ability of the optical properties to classify different categories of bacteria.

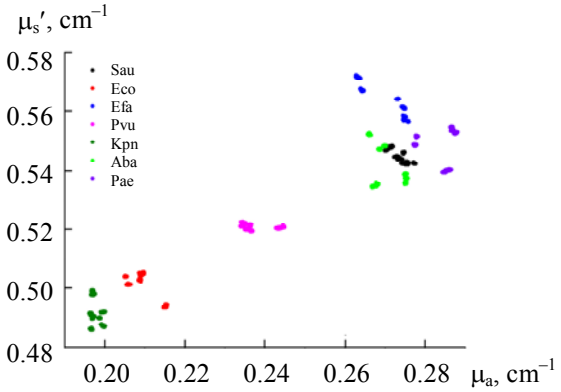

Fig. 5. Scatter plot of the optical properties at the 1450 nm wavelength for seven categories of bacteria.

The parameters of an SVM have a great influence on the classification result, so PSO can be applied to optimize the parameters. To validate the performance of PSO, it was compared with a default SVM method. The kernel functions of the SVM, including linear, polynomial and RBF, were also compared, and recorded as SVML, SVMP, and SVMR, respectively. To avoid randomness, the experiments were repeated 10 times, and the average accuracy value was recorded. The classification results for each category of bacteria and the overall classification result (OCR) and average classification result (ACR) for the seven categories of bacteria are shown in Table 2. Although the ACR and OCR of SVML were 96.99% and 96.98%, respectively, the

classification accuracy of Aba was approximately 78%. The ACR and OCR of SVMP and SVMR were less than 35%. Therefore, it was difficult for the default SVM method to classify the bacteria, and its generalization ability was poor. As can be seen, the classification results of the model optimized by PSO improved a great deal. The optimized polynomial kernel function of the SVM (PSO-SVMP) method demonstrated good performance, achieving a prediction ability of 100% for every category of bacteria. The ACR and OCR of PSO-SVML and PSO-SVMR were over 99%.

TABLE 2. Classification Result, OCR, and ACR (in %) for SVML, SVMP, and SVMR with the Default Parameter and PSO

Bacteria	SVML	SVMP	SVMR	PSO-SVML	PSO-SVMP	PSO-SVMR
Sau	100.00	0	4.64	100.00	100.00	100.00
Eco	100.00	0	3.92	100.00	100.00	100.00
Efa	100.00	0	3.89	100.00	100.00	100.00
Pvu	100.00	0	62.31	100.00	100.00	100.00
Kpn	100.00	0	4.69	100.00	100.00	99.85
Aba	78.91	0	4.48	94.34	100.00	100.00
Pae	100.00	100.00	91.33	100.00	100.00	100.00
ACR	96.99	14.29	25.25	99.19	100.00	99.97
OCR	96.98	19.99	31.21	99.19	100.00	99.97

The results indicate that the PSO-SVM method was able to adequately distinguish the seven categories of bacteria based on the optical properties of NIDRS. The PSO-SVM method demonstrated good generalization performance at a significantly high classification accuracy, which has great potential to be applied in clinical burn wound bacteria classification. The favorable results of PSO-SVM demonstrate that optical properties can be used to classify and discriminate pathogenic bacteria.

Conclusion. Near-infrared diffuse reflectance spectroscopy was proposed for the classification of burn wound bacteria based on reduced scattering coefficient μ_s' and absorption coefficient μ_a, which reflect the structure and composition of bacteria. They can fundamentally differentiate different categories of bacteria. A default SVM and PSO-SVM classifiers were applied to prove that the optical properties were efficient for bacterial classification. It was difficult for the default SVM to obtain high classification accuracy for seven categories of bacteria, and it demonstrated poor generalization performance. Despite this, combined with PSO, the PSO-SVM classifier based on the optical properties achieved favorable classification results. The method based on the NIDRS system is noninvasive, noncontact, and effective. The model provides an insight into the optical properties that discriminate different categories of bacteria. An in-depth analysis of the optical properties revealed the internal structure and composition of the bacteria, and explored the essential differences between the different types of pathogenic bacteria. In the future, this system could be used to establish a database of optical properties for different bacteria, which would provide a promising tool for the rapid and noninvasive classification of burn wound bacteria with high reproducibility.

This research was funded by the National Natural Science Foundation of China NSFC (No. 61771080, 81701904, 61571069), the Fundamental and Advanced Research Project of Chongqing (cstc2016jcyjA0043, cstc2016jcyjA0134), Chongqing Social Undertaking and People's Livelihood Guarantee Science and Technology innovation Special Foundation (cstc2016shmszx0111), and the Open Project Program of the National Laboratory of Pattern Recognition (NLPR)(201800011).

REFERENCES

1. J. Q. Nguyen, C. Crouzet, T. Mai, K. Riola, D. Uchitel, L. H. Liaw, N. Bernal, A. Ponticorvo, B. Choi, A. J. Durkin, *J. Biomed. Opt.*, **18**, 66010 (2013).
2. S. Demesquita, L. H. Aulick, K. A. Burgess, *Physiol. Behav.*, **51**, 363–369 (1992).
3. J. P. Barret, D. N. Herndon, *Plast. Reconstr. Surg.*, **111**, 744–750 (2003).
4. J. L. de Macedo, J. B. Santos, *Mem. Inst. Oswaldo Cruz*, **100**, 535–539 (2005).
5. B. R. Sharma, *Infect. Dis. Clin. N. Am.*, **21**, 745–759 (2007).
6. M. Ahmad, H. S. Shahid, K. M. Ibrahim, S. A. Malik, *Ann. Burns Fire Disasters.*, **19**, 18 (2006).
7. J. He, Z. Liu, Y. Xiao, X. Fan, J. Yan, H. P. Liang, *Burns Trauma.*, **2**, 106–113 (2014).

8. J. G. Hughes, E. A. Vetter, R. Patel, C. D. Schleck, S. Harmsen, L. T. Turgeant, F. R. Cockerill III, *J. Clin. Microbiol.*, **39**, 4468–4471 (2002).
9. A. Velay, F. Schramm, J. Gaudias, B. Jaulhac, P. Riegel, *Diagn. Microbiol. Infect. Dis.*, **68**, 83–85 (2010).
10. M. A. Jensen, J. A. Webster, N. Straus, *Appl. Environ. Microbiol.*, **59**, 945–952 (1993).
11. H. Liu, W. Liu, X. Yang, X. Zhou, D. Xing, *Anal. Chem.*, **88**, 10191–10197 (2016).
12. J. Shen, Y. Guan, J. Zhang, J. Tang, X. Lu, C. Zhang, *Exp. Ther. Med.*, **7**, 496–500 (2014).
13. N. Massadivanir, G. Shtenberg, E. Segal, *J. Vis. Exp.*, **81**, e50805 (2013).
14. T. Belal, K. Romdhane, B. Jean-Louis, B. Tahar, D. Eric, L. Françoise, *Anal. Methods.*, **3**, 133–143 (2011).
15. L. E. Rodriguezsaona, F. M. Khambaty, F. S. Fry, E. M. Calvey, *J. Agric. Food Chem.*, **49**, 574–579 (2001).
16. K. Maquelin, C. Kirschner, L. P. Choosmith, N. A. Ngothi, V. T. Van, M. Stämmler, H. P. Endtz, H. A. Bruining, D. Naumann, G. J. Puppels, *J. Clin. Microbiol.*, **41**, 324–329 (2003).
17. A. C. Samuels, A. P. Snyder, D. K. Emge, D. Amant, J. Minter, M. Campbell, A. Tripathi, *Appl. Spectrosc.*, **63**, 14–24 (2009).
18. P. Żarnowiec, Ł. Lechowicz, G. Czerwonka, W. Kaca, *Curr. Med. Chem.*, **22**, 1710–1718 (2015).
19. A. D. S. Marques, J. T. N. Nicácio, T. A. Cidral, M. C. N. D. Melo, K. M. G. D. Lima, *J. Microbiol. Methods*, **93**, 90–94 (2013).
20. M. C. Skala, G. M. Palmer, K. M. Vrotsos, A. Gendronfitzpatrick, N. Ramanujam, *Opt. Express*, **15**, 7863–7875 (2007).
21. P. P. Banada, K. Huff, E. Bae, B. Rajwa, A. Aroonnual, B. Bayraktar, A. Adil, J. P. Robinsond, E. D. Hirleman, A. K. Bhunia, *Biosens. Bioelectron.*, **24**, 1685–1692 (2008).
22. Y. Jo, J. Jung, M. H. Kim, H. Park, S. J. Kang, Y. K. Park, *Opt. Express*, **23**, 15792–15805 (2015).
23. G. Zonios, L. T. Perelman, V. Backman, R. Manoharan, M. Fitzmaurice, D. J. Van, S. F. Michael, *Appl. Opt*., **38**, 6628 (1999).
24. B. Acha, C. Serrano, S. Palencia, J. J. Murillo, *Proc. SPIE*, **5370**, 1018–1025 (2004).
25. Q. H. He, J. Yan, Y. Shen, Y. T. Bi, G. H. Ye, F. C. Tian, Z. G. Wang, *Intell. Autom. Soft Comp.*, **18**, 967–979 (2012).